

Influence of the deviation of the matter power spectrum at small scales on the global 21-cm signal at cosmic dawn

Yupeng Yang^{1,*}, Xiujuan Li^{2,†} and Gang Li^{1,‡}

¹*School of Physics and Physical Engineering, Qufu Normal University, Qufu, Shandong, 273165, China*

²*School of Cyber Science and Engineering, Qufu Normal University, Qufu, Shandong, 273165, China*



(Received 11 October 2022; accepted 20 April 2023; published 4 May 2023)

The matter power spectrum has been strongly constrained by astronomical measurements at large scales, but only weakly at small scales. Compared with the standard scenario, the deviation of the matter power spectrum at small scales has influence on the cosmological structure formation, e.g., the comoving number density of dark matter halos. The thermal history of the intergalactic medium (IGM) can be changed if dark matter is made of weakly interacting massive particles and can annihilate into standard model particles. The changes of the evolution of IGM could leave imprints on the relevant astronomical observations. Taking into account the dark matter annihilation, we investigate the impact of the deviation of matter power spectrum at small scales on the global 21-cm signal. In view of the measurements of the global 21-cm signal by the EDGES experiment, we explore the allowed parameter space of m_s , which describes the degree of deviation, by requiring the differential brightness temperature of the global 21-cm signal $\delta T_{21} \leq -50$ mK at redshift $z = 17$.

DOI: [10.1103/PhysRevD.107.103501](https://doi.org/10.1103/PhysRevD.107.103501)

I. INTRODUCTION

The standard inflation model has predicted that the primordial power spectrum is in a scale invariant form of $\mathcal{P}(k) \sim k^{n_s-1}$ [1–5]. At large scales, $10^{-4} \lesssim k \lesssim 1 \text{ Mpc}^{-1}$, primordial power spectrum has been well constrained by astronomical measurements, e.g., cosmic microwave background (CMB), large-scale structure and Lyman- α forest [6–8]. At small scales, $k \gtrsim 1 \text{ Mpc}^{-1}$, the constraints are from the studies of, e.g., primordial black holes, ultra-compact minihalos, galaxy luminosity functions and Silk damping effects [9–19]. The primordial power spectrum results in a matter power spectrum $P_m(k) \sim k^{n_s}$. The astronomical measurements such as CMB have been used to reconstruct the matter power spectrum at large scales $10^{-3} \lesssim k \lesssim 0.19 \text{ Mpc}^{-1}$ [20]. Large-scale 21-cm measurements could be used to probe the matter power spectrum at small scales [21]. Any deviation of $P_m(k)$ at small scales can result in the changes of the cosmological structure formation such as the comoving number density of dark matter halos, while no conflict with existing astronomical measurements [22–25].

The existence of dark matter (DM) has been confirmed by many different astronomical observations. However, the nature of DM still keeps unknown. Different DM models have been proposed and one of the mostly studied is weakly

interacting massive particles (WIMPs) [26,27]. The relevant theory proposes that WIMPs can annihilate into standard model particles such as electrons, positrons and photons. These particles have interactions with that existing in the Universe, resulting in the changes of the thermal history of intergalactic medium (IGM) [28–43]. These changes could leave imprints on different astronomical observations such as the CMB and global 21-cm signal. Furthermore, the properties of DM can be investigated by the relevant astronomical measurements; see, e.g., Refs. [30–32,35–37,44,45].

As mentioned above, the deviation of the matter power spectrum at small scales can lead to the changes of the comoving number density of DM halos. Taking into account the DM annihilation, it is expected that the deviation can lead to the different thermal history of the IGM and astronomical observations compared with the standard scenario. The authors of [24] have investigated these effects on the CMB observations. In this work, following the methods in [24] we will study the impact of the deviation of matter power spectrum at small scales on the global 21-cm signal in the cosmic dawn.

As an important way to study the early universe, the detection of the global 21-cm signal is very challenging [46,47]. Recently, the experiment to detect the global epoch of reionization signature (EDGES) reported their results of the global 21-cm signal [48]. They found an absorption signal centered at redshift $z \sim 17$ about twice as large as expected [47,49,50]. Note that the results of the EDGES experiment are still controversial and require further

*ypyang@aliyun.com

†lxj@qfnu.edu.cn

‡gli@qfnu.edu.cn

verification [51–54]. On the other hand, the global 21-cm signal can be used to investigate the properties of DM; see, e.g., Refs. [35–39,42,55–65]. In this paper, taking into account the DM annihilation and by requiring the differential brightness temperature of the global 21-cm signal, e.g., $\delta T_{21} \lesssim -50$ mK at redshift $z = 17$, we explore the parameter space of m_s , which characterizes the deviation of the matter power spectrum at small scales. Here we have not included the heating effects from astrophysical processes performed in the standard scenario [50,66–68].

This paper is organized as follows. In Sec. II we present the basically related components of the matter power spectrum considered here, and the basic equations for the evolution of the IGM including DM annihilation. In Sec. III, we investigate the impact of the deviation of matter power spectrum at small scales on the global 21-cm signal, and then explore the allowed space of the related parameter. The conclusions are given in Sec. IV. Throughout the paper we will use the cosmological parameters from Planck-2018 results [4].

II. THE MATTER POWER SPECTRUM AT SMALL SCALES AND THE EVOLUTION OF IGM

In the standard scenario, the matter power spectrum resulted from the primordial power spectrum is in a form of $P_m(k) \sim k^{n_s}$. Many other inflation models have been proposed and suggested that the primordial power spectrum could be deviated at small scales while being consistent with existing astronomical measurements at large scales. For the most inflation models, the deviation of $\mathcal{P}(k)$ is suggested in a form of power law growth at small scales; see, e.g., Refs. [69–76]. In view of these factors, following Ref. [24], we take the parametrized form of the matter power spectrum as follows

$$P_m(k) = \begin{cases} A_m k^{n_s} & k \leq k_p \\ A_m k_p^{n_s} \left(\frac{k}{k_p}\right)^{m_s} & k > k_p \end{cases} \quad (1)$$

where the pivot scale $k_p \gtrsim 10 \text{ Mpc}^{-1}$ in order to be consistent with the available astronomical observations. The matter power spectrum at redshift z can be written as

$$P_m(z, k) = P_m(k) T^2(k) \frac{D^2(z)}{D^2(0)}, \quad (2)$$

where $D(z)$ is the growth factor [77,78], and $T(k)$ is transfer function [79]. A_m is a constant normalized as $\sigma_8 = 0.8$, where σ_8 is the root mean square mass fluctuation in a sphere of radius $8h^{-1} \text{ Mpc}$. The mass variance $\sigma^2(z)$ is written as follows

$$\sigma^2(z, M) = \int \frac{dk k^3 P_m(z, k)}{k 2\pi^2} W^2(kR), \quad (3)$$

where $W(x)$ is the window function and we use the form as

$$W(x) = \frac{3(\sin x - x \cos x)}{x^3}. \quad (4)$$

Since the changes of $P_m(k)$ investigated here are mainly on small scales, nonlinear effects are very important. There are several ways to deal with nonlinear effects. For the purpose of this work, one way is using the Zeldovich approximation or Lagrangian perturbation theory [80–82]. Another way is using the Press-Schechter (PS) theory [83], which has been proved to be valid and widely used in literature; see, e.g., Refs. [84–86]. The evolution of nonlinear effects will result in the collapse of the regions with large density perturbation. Although on small scales the mass variance σ^2 calculated using the linear power spectrum is different from that of nonlinear power spectrum, PS theory shows that the collapsed fraction can be obtained using the linear power spectrum. In this work, we will use PS theory to deal with nonlinear effects on small scales. On the other hand, since we mainly focused on the effects of dark matter annihilation within dark matter halos, there is another method of calculating the “boost factor” (BF) to deal with nonlinear effects. The BF can be obtained by directly integrating the nonlinear matter power spectrum for investigated scales at different redshifts [60,87,88]. Essentially, this method is the same as the PS theory.

For the Press-Schechter mass function, the comoving number density of DM halos is in a form of [89]

$$\frac{dn(z, M)}{dM} = \sqrt{\frac{2}{\pi}} \frac{\rho_0 \delta_c}{M \sigma^2} \frac{d\sigma}{dM} \exp\left(-\frac{\delta_c^2}{2\sigma^2}\right), \quad (5)$$

where $\delta_c = 1.686$ is the threshold for spherical collapse. In Fig. 1, we plot the comoving number density of DM halos for different values of $m_s = 1.30$ and 1.60 at redshift $z = 15$ for pivot scale $k_p = 100 \text{ Mpc}^{-1}$. For comparison,

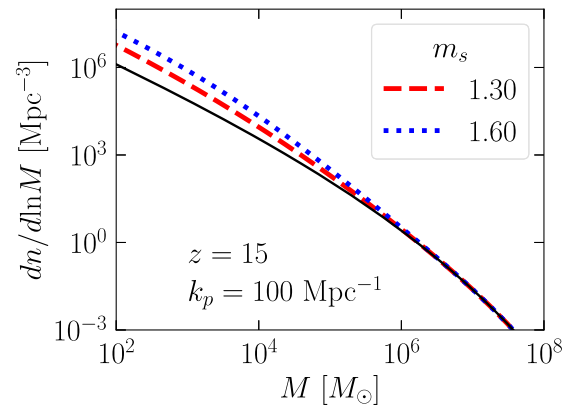


FIG. 1. Comoving number density of dark matter halos for different values of $m_s = 1.30$ and 1.60 at redshift $z = 15$ for the pivot scale $k_p = 100 \text{ Mpc}^{-1}$. We also plot the standard scenario for comparison ($m_s = n_s = 0.96$, thin solid black line).

we also plot the standard scenario with $m_s = n_s = 0.96$ [4]. From this plot, it can be seen that the deviation of the matter power spectrum at small scales results in an increase of the comoving number density of DM halos with small masses. Since we have set the pivot scale $k_p = 100 \text{ Mpc}^{-1}$, compared with the standard scenario, the significant difference appears for the masses of $M \lesssim 6 \times 10^5 M_\odot$.

Taking into account the DM annihilation, the energy release rate per unit volume can be written as [24,29–31,37,90]

$$\left. \frac{dE}{dV dt} \right|_{\text{DM}} = (1+z)^3 \frac{\langle \sigma v \rangle}{m_\chi} \int dM \frac{dn}{dM} \int 4\pi r^2 \rho_\chi^2(r) dr, \quad (6)$$

where $\langle \sigma v \rangle$ is the thermally averaged cross section of DM annihilation, and m_χ is the mass of DM particle. $\rho_\chi(r)$ is the density profile of DM halos and we adopt the Navarro-Frenk-White model for our calculations [91].

The energy released from DM annihilation can inject into the Universe resulting in the changes of the thermal history of IGM. The evolutions of the ionization fraction x_e and kinetic temperature T_k of the IGM are governed by the following equations [11,29,32,92]:

$$(1+z) \frac{dx_e}{dz} = \frac{1}{H(z)} [R_s(z) - I_s(z) - I_{\text{DM}}(z)], \quad (7)$$

$$(1+z) \frac{dT_k}{dz} = \frac{8\sigma_T a_R T_{\text{CMB}}^4 x_e (T_k - T_{\text{CMB}})}{3m_e c H(z) (1 + f_{\text{He}} + x_e)} - \frac{2}{3k_B H(z)} \frac{K_{\text{DM}}}{1 + f_{\text{He}} + x_e} + 2T_k, \quad (8)$$

where $R_s(z)$ is the standard recombination rate, $I_s(z)$ is the ionization rate by standard sources. I_{DM} and K_{DM} are the ionization and heating rate by DM annihilation, which can be written as follows [11,29,32,59,92]:

$$I_{\text{DM}} = f_i(z) \frac{1}{n_b} \frac{1}{E_0} \left. \frac{dE}{dV dt} \right|_{\text{DM}}, \quad (9)$$

$$K_{\text{DM}} = f_h(z) \frac{1}{n_b} \left. \frac{dE}{dV dt} \right|_{\text{DM}}, \quad (10)$$

where n_b stands for the baryon number density and $E_0 = 13.6 \text{ eV}$. $f(z)$ is the fraction of the energy released from DM annihilation injected into the IGM for ionization and heating, respectively. Here we have used the public code ExoCLASS [93], a branch of the public code CLASS [94], to calculate $f(z)$ numerically.

III. THE IMPACT OF THE DEVIATION ON THE GLOBAL 21-cm SIGNAL AND CORRESPONDING CONSTRAINTS

The quantity associated with the observations describing the global 21-cm signal is the differential brightness

temperature δT_{21} . Relative to the CMB background, δT_{21} can be written as follows [38,42,95]

$$\delta T_{21} = 16(1-x_e) \left(\frac{\Omega_b h}{0.02} \right) \left(\frac{1+z \cdot 0.3}{10 \Omega_m} \right)^{\frac{1}{2}} \times \left(1 - \frac{T_{\text{CMB}}}{T_s} \right) \text{ mK}, \quad (11)$$

where Ω_b and Ω_m are the density parameters of baryonic matter and DM, respectively. h is the reduced Hubble constant. T_s is the spin temperature, which is mainly effected by background photons, collisions between the particles and resonant scattering of Ly α photons (Wouthuysen-Field effect) [46,47]. Taking into account these factors and with CMB as main background, the spin temperature can be written as follows [28,42]:

$$T_s = \frac{T_{\text{CMB}} + (y_\alpha + y_c) T_k}{1 + y_\alpha + y_c}, \quad (12)$$

where y_α is related to the Wouthuysen-Field effect and we adopt the formula used in, e.g., Refs. [11,28,96]:

$$y_\alpha = \frac{P_{10} T_\star}{A_{10} T_k} \exp \left[-\frac{0.3(1+z)^{\frac{1}{2}}}{T_k^{\frac{2}{3}} (1 + \frac{0.4}{T_k})} \right], \quad (13)$$

where $A_{10} = 2.85 \times 10^{-15} \text{ s}^{-1}$ is the Einstein coefficient of hyperfine spontaneous transition. $T_\star = 0.068 \text{ K}$ corresponds to the energy changes between triplet and singlet states of neutral hydrogen atom. P_{10} is the radiative deexcitation rate due to Ly α photons [46,47]. The factor y_c involves collisions between hydrogen atoms and other particles [28,38,43,96,97],

$$y_c = \frac{(C_{\text{HH}} + C_{\text{eH}} + C_{\text{pH}}) T_\star}{A_{10} T_k}, \quad (14)$$

where $C_{\text{HH,eH,pH}}$ are the deexcitation rate due to collisions and the fitted formulas can be found in Refs. [38,43,96,97].

In order to explore the conservative allowed space of relevant parameter, following previous works [37,59], here we have not included any astrophysical heating source. The main astrophysical source affecting the global 21-cm signal is the Ly α photons related to the Wouthuysen-Field effect [47,59,98–103]. Here we have considered that the Ly α photons are mainly from Pop II stars. We take the virial temperature of a halo $T_{\text{vir}} = 10^4 \text{ K}$ corresponding to the minimum halo mass. For the star formation efficiency f_\star , we have set $f_\star = 0.05$ for our calculations, and we found that larger f_\star will slightly increase the amplitude of δT_{21} at redshift $z = 17$. We take the total number of photons from the Pop II stars between the Ly α and the Lyman limits as $N_{\text{tot}} = 9690$. Based on these choices, we can obtain the

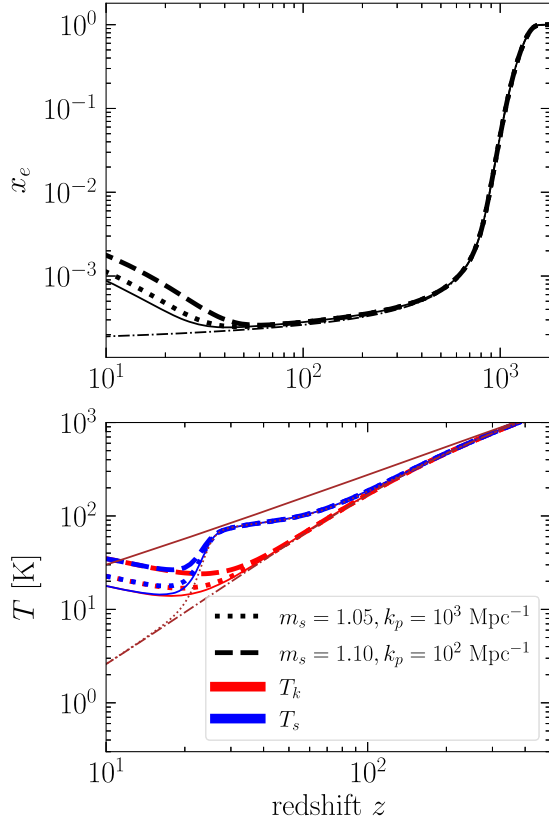


FIG. 2. The evolution of x_e , T_k , and T_s with redshift z for different values of m_s and k_p . Here we have set $m_\chi = 100$ GeV and $\langle\sigma v\rangle = 3 \times 10^{-26} \text{ cm}^{-3} \text{ s}^{-1}$. We also plot the standard scenario for comparison ($m_s = n_s = 0.96$, thin solid lines). The case without standard astrophysical heating sources is also shown (x_e : thin dot-dashed black line, T_k : thin dot-dashed brown line, T_s : thin dotted brown line). The temperature of CMB is also shown in the thin solid brown line.

global 21-cm signal at redshift $z = 17$ with the maximum amplitude allowed within a reasonable range of parameters.

After deriving the energy release rate per unit volume due to DM annihilation as shown in Eq. (6), one can get the changes of x_e , T_k and T_s with redshift z using Eqs. (7), (8), and (12). In order to include the effects of DM annihilation, we have modified the public code RECFAST in CAMB¹ to solve the differential equations numerically [11,12,29,32,59,92]. Then the differential brightness temperature δT_{21} can be obtained with Eq. (11). In Fig. 2, we plot the evolution of x_e , T_k , and T_s for different values of m_s and k_p . Compared with the standard scenario ($m_s = n_s = 0.96$, thin solid lines), the ionization fraction, kinetic temperature, and spin temperature are all increased. Here we have set the canonical value of DM annihilation cross section as $\langle\sigma v\rangle = 3 \times 10^{-26} \text{ cm}^{-3} \text{ s}^{-1}$ and $b\bar{b}$ channel for our calculations.

¹<https://camb.info/>.

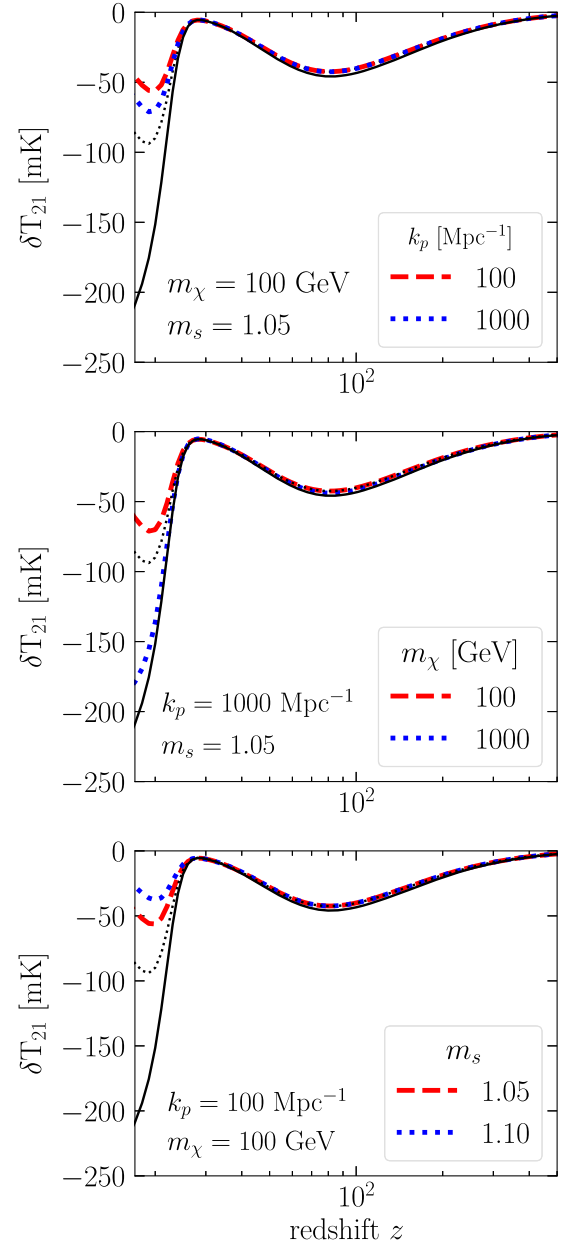


FIG. 3. The evolution of differential brightness temperature δT_{21} with redshift z for different values of k_p , m_χ , and m_s . We have set $\langle\sigma v\rangle = 3 \times 10^{-26} \text{ cm}^{-3} \text{ s}^{-1}$ and $b\bar{b}$ channel for our calculations. For comparison, we also show the case without any heating sources (thin solid black line) and the case for the standard matter power spectrum $m_s = n_s$ with DM annihilation ($m_\chi = 100$ GeV, thin dotted black line).

In Fig. 3, the evolution of δT_{21} for different values of k_p , m_χ , and m_s are shown, respectively. For comparison, we also plot the default case with no DM annihilation (thin solid black line) and the standard case with no deviation of the matter power spectrum at small scales (thin dotted black line). For fixed DM mass m_χ and power law index of the deviation m_s (top panel in Fig. 3), smaller pivot scale results in an increase of the number density of DM halos at

small masses. Therefore, the absorption amplitude of the global 21-cm signal is reduced compared with the standard scenario. For fixed pivot scale k_p and power law index of the deviation m_s (middle panel in Fig. 3), lighter DM corresponds to a larger DM number density. Since the DM annihilation rate is proportional to the squared number density, much more energy is injected into the IGM, causing a reduction of the absorption amplitude of the global 21-cm signal. For fixed pivot scale k_p and DM mass m_χ (bottom panel in Fig. 3), larger power law index of the deviation m_s also results in an increase of the number density of DM halos at small masses. Similar to the case of changing pivot scale, the absorption amplitude of the global 21-cm signal is decreased for larger m_s compared with the scenario of no deviation.

In view of the results of the EDGES experiment, by requiring the differential brightness temperature $\delta T_{21} \leq -50$ mK at redshift $z = 17$, we explore the allowed space of parameter m_s for different pivot scales $k_p = 10, 100$, and 1000 Mpc^{-1} , which is shown in Fig. 4. From this plot, it can be seen that smaller DM mass or pivot scale corresponds to a smaller value of m_s . In Ref. [24], the authors derived the upper limits on m_s using the CMB observations. They found that for the parameter $f\langle\sigma v\rangle/m_\chi = 3 \times 10^{-28} \text{ cm}^3 \text{ s}^{-1} \text{ GeV}^{-1}$, the upper limit is $m_s = 1.43(1.63)$ for $k_p = 100(1000)h \text{ Mpc}^{-1}$, and it is roughly weaker than our result for the DM mass range considered here.

Note that here we have not included the standard astrophysical heating sources, e.g., the x ray from stars, which can also heat the IGM and result in the increase of x_e , T_k , and T_s in lower redshifts [28,46,47]. For this case, compared with our results, the amplitude of differential

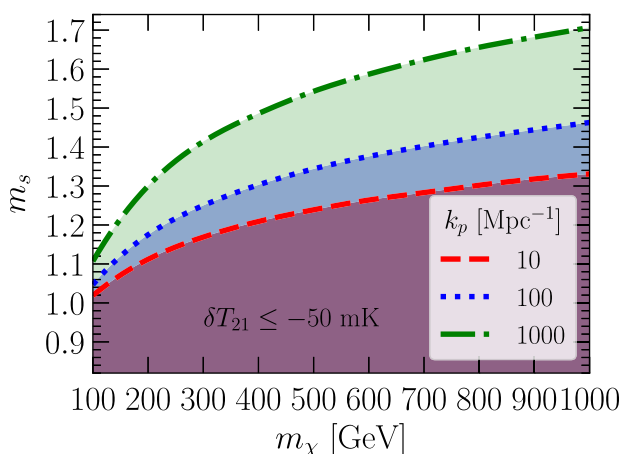


FIG. 4. The allowed space of parameter m_s (shaded areas) for different pivot scales $k_p = 10, 100$, and 1000 Mpc^{-1} by requiring the differential brightness temperature $\delta T_{21} \leq -50$ mK. We have set $\langle\sigma v\rangle = 3 \times 10^{-26} \text{ cm}^3 \text{ s}^{-1}$ and $b\bar{b}$ channel for our calculations.

brightness temperature δT_{21} at redshift $z = 17$ will become smaller, resulting in a lower allowed value of m_s .

In this work, we have used the canonical value of DM annihilation cross section for our calculations. Many astronomical observations have been used to constrain $\langle\sigma v\rangle$ depending on the DM mass [104–108]. The authors of [105], for instance, have used the Planck-2018 datasets to get the constraints and found $\langle\sigma v\rangle \lesssim 3 \times 10^{-25}(10^{-24}) \text{ cm}^3 \text{ s}^{-1}$ for $m_\chi = 100(1000) \text{ GeV}$. As shown in Eq. (6), larger value of $\langle\sigma v\rangle$ will result in the larger energy release rate per unit volume, and it is expected that the final allowed value of m_s will become smaller.

Note that the final allowed space of parameter m_s can be effected by relevant parameters, and these parameters would be degenerate with each other. A complete way to deal with this issue is combining the observed data of the EDGES to obtain the distribution and correlation of parameters by using the MCMC method. We will address this issue in future work.

IV. CONCLUSIONS

In the standard scenario, the matter power spectrum has a form of $P_m(k) \sim k^{n_s}$. Many relevant theories indicate that the matter power spectrum could be deviated at small scales while being consistent with the available astronomical observations. In this work, we have investigated the impact of this kind of deviation on the global 21-cm signal in the cosmic dawn, taking into account DM annihilation. Specifically, we have adopted a power law growth of the matter power spectrum at small scales, $P_m \sim k_p^{n_s} (k/k_p)^{m_s}$ for $k > k_p \simeq 10 \text{ Mpc}^{-1}$. The deviation of the matter power spectrum at small scales results in an increase of the comoving number density of DM halos at small masses. The energy release rate per unit volume due to DM annihilation becomes larger compared with the standard scenario, resulting in the changes of the thermal history of IGM and then the evolution of the global 21-cm signal. The absorption amplitude of the global 21-cm signal is reduced for smaller pivot scale k_p or larger power law index m_s . Smaller DM mass m_χ can also decrease the absorption amplitude of the global 21-cm signal due to the larger annihilation rate. In view of the results of the EDGES experiment, we have explored the allowed parameter space of the power law index m_s for different pivot scales by requiring the differential brightness temperature $\delta T_{21} \leq -50$ mK. Smaller DM mass or pivot scale results in a lower allowed value of m_s . For a DM mass, e.g., $m_\chi = 100(1000) \text{ GeV}$, the largest allowed value is $m_s = 1.05(1.46)$ for the pivot scale $k_p = 100 \text{ Mpc}^{-1}$.

Note that we have considered the global 21-cm signal in the cosmic dawn that can be influenced by many other astrophysical factors. The global 21-cm signal in the dark

ages ($30 \lesssim z \lesssim 300$) can also be effected by the deviation of the matter power spectrum at small scales. Compared with the standard scenario, the global 21-cm signal in the dark ages is very little influenced by the astrophysical processes. Therefore, it is expected that the future detection of the global 21-cm signal (or the 21-cm power spectrum) in the dark ages by, e.g., the radio telescopes on the moon or satellites around a low lunar orbit [58,109–113], could give better constraints on the deviation of the matter power spectrum at small scales.

ACKNOWLEDGMENTS

We thank Bin Yue for very useful discussions. Y. Y. is supported by the Shandong Provincial Natural Science Foundation (Grant No. ZR2021MA021). X. L. is supported by the Youth Innovations and Talents Project of Shandong Provincial Colleges and Universities (Grant No. 201909118). G. L. is supported by the Taishan Scholar Project of Shandong Province (Grant No. tsqn202103062). The authors would like to thank the anonymous referees for their very helpful comments and suggestions.

-
- [1] J. E. Lidsey, A. R. Liddle, E. W. Kolb, E. J. Copeland, T. Barreiro, and M. Abney, Reconstructing the inflaton potential—an overview, *Rev. Mod. Phys.* **69**, 373 (1997).
 - [2] D. S. Salopek, J. R. Bond, and J. M. Bardeen, Designing density fluctuation spectra in inflation, *Phys. Rev. D* **40**, 1753 (1989).
 - [3] M. Joy, V. Sahni, and A. A. Starobinsky, New universal local feature in the inflationary perturbation spectrum, *Phys. Rev. D* **77**, 023514 (2008).
 - [4] N. Aghanim *et al.* (Planck Collaboration), Planck 2018 results. VI. Cosmological parameters, *Astron. Astrophys.* **641**, A6 (2020).
 - [5] S. M. Leach, Measuring the primordial power spectrum: Principal component analysis of the cosmic microwave background, *Mon. Not. R. Astron. Soc.* **372**, 646 (2006).
 - [6] R. Hlozek *et al.*, The atacama cosmology telescope: A measurement of the primordial power spectrum, *Astrophys. J.* **749**, 90 (2012).
 - [7] S. Bird, H. V. Peiris, M. Viel, and L. Verde, Minimally parametric power spectrum reconstruction from the lyman α forest, *Mon. Not. R. Astron. Soc.* **413**, 1717 (2011).
 - [8] J. L. Tinker, E. S. Sheldon, R. H. Wechsler, M. R. Becker, E. Rozo, Y. Zu, D. H. Weinberg, I. Zehavi, M. R. Blanton, M. T. Busha, and B. P. Koester, Cosmological constraints from galaxy clustering and the mass-to-number ratio of galaxy clusters, *Astrophys. J.* **745**, 16 (2012).
 - [9] A. S. Josan, A. M. Green, and K. A. Malik, Generalised constraints on the curvature perturbation from primordial black holes, *Phys. Rev. D* **79**, 103520 (2009).
 - [10] I. Dalianis, Constraints on the curvature power spectrum from primordial black hole evaporation, *J. Cosmol. Astropart. Phys.* **08** (2019) 032.
 - [11] Y. Yang, Constraints on the small scale curvature perturbation using Planck-2015 data, *Mon. Not. R. Astron. Soc.* **486**, 4569 (2019).
 - [12] Y. Yang, Constraints on primordial black holes and curvature perturbations from the global 21-cm signal, *Phys. Rev. D* **102**, 083538 (2020).
 - [13] H. A. Clark, G. F. Lewis, and P. Scott, Investigating dark matter substructure with pulsar timing. II. Improved limits on small-scale cosmology, *Mon. Not. R. Astron. Soc.* **456**, 1402 (2016); **464**, 955(E) (2017).
 - [14] T. Bringmann, P. Scott, and Y. Akrami, Improved constraints on the primordial power spectrum at small scales from ultracompact minihalos, *Phys. Rev. D* **85**, 125027 (2012).
 - [15] Y. Yang and Y. Qin, Tau neutrinos from ultracompact dark matter minihalos and constraints on the primordial curvature perturbations, *Phys. Rev. D* **96**, 103509 (2017).
 - [16] F. Li, A. L. Erickcek, and N. M. Law, A new probe of the small-scale primordial power spectrum: Astrometric microlensing by ultracompact minihalos, *Phys. Rev. D* **86**, 043519 (2012).
 - [17] D. Jeong, J. Pradler, J. Chluba, and M. Kamionkowski, Silk Damping at a Redshift of a Billion: A New Limit on Small-Scale Adiabatic Perturbations, *Phys. Rev. Lett.* **113**, 061301 (2014).
 - [18] S. Yoshiura, M. Oguri, K. Takahashi, and T. Takahashi, Constraints on primordial power spectrum from galaxy luminosity functions, *Phys. Rev. D* **102**, 083515 (2020).
 - [19] D. Jeong, J. Pradler, J. Chluba, and M. Kamionkowski, Silk Damping at a Redshift of a Billion: New Limit on Small-Scale Adiabatic Perturbations, *Phys. Rev. Lett.* **113**, 061301 (2014).
 - [20] R. Hlozek *et al.*, The Atacama Cosmology Telescope: A measurement of the primordial power spectrum, *Astrophys. J.* **749**, 90 (2012).
 - [21] J. B. Muñoz, C. Dvorkin, and F.-Y. Cyr-Racine, Probing the small-scale matter power spectrum with large-scale 21-cm data, *Phys. Rev. D* **101**, 063526 (2020).
 - [22] P. Villanueva-Domingo and K. Ichiki, 21 cm forest constraints on primordial black holes, *Publ. Astron. Soc. Jpn.* **75**, S33 (2023).
 - [23] H. Tashiro and N. Sugiyama, The effect of primordial black holes on 21 cm fluctuations, *Mon. Not. R. Astron. Soc.* **435**, 3001 (2013).
 - [24] A. Natarajan, N. Zhu, and N. Yoshida, Probing the small scale matter power spectrum through dark matter annihilation in the early Universe, [arXiv:1503.03480](https://arxiv.org/abs/1503.03480).
 - [25] S. Yoshiura, K. Takahashi, and T. Takahashi, Impact of EDGES 21-cm global signal on the primordial power spectrum, *Phys. Rev. D* **98**, 063529 (2018).
 - [26] G. Bertone, D. Hooper, and J. Silk, Particle dark matter: Evidence, candidates and constraints, *Phys. Rep.* **405**, 279 (2005).

- [27] G. Jungman, M. Kamionkowski, and K. Griest, Super-symmetric dark matter, *Phys. Rep.* **267**, 195 (1996).
- [28] Q. Yuan, B. Yue, X.-J. Bi, X. Chen, and X. Zhang, Leptonic dark matter annihilation in the evolving universe: Constraints and implications, *J. Cosmol. Astropart. Phys.* **10** (2010) 023.
- [29] X. Chen and M. Kamionkowski, Particle decays during the cosmic dark ages, *Phys. Rev. D* **70**, 043502 (2004).
- [30] L. Zhang, X.-L. Chen, Y.-A. Lei, and Z.-G. Si, The impacts of dark matter particle annihilation on recombination and the anisotropies of the cosmic microwave background, *Phys. Rev. D* **74**, 103519 (2006).
- [31] M. S. Madhavacheril, N. Sehgal, and T. R. Slatyer, Current dark matter annihilation constraints from CMB and low-redshift data, *Phys. Rev. D* **89**, 103508 (2014).
- [32] Y. Yang, Constraints on the basic parameters of dark matter using the Planck data, *Phys. Rev. D* **91**, 083517 (2015).
- [33] T. R. Slatyer, Indirect dark matter signatures in the cosmic dark ages II. Ionization, heating and photon production from arbitrary energy injections, *Phys. Rev. D* **93**, 023521 (2016).
- [34] K. Cheung, J.-L. Kuo, K.-W. Ng, and Y.-L. S. Tsai, The impact of EDGES 21-cm data on dark matter interactions, *Phys. Lett. B* **789**, 137 (2019).
- [35] E. D. Kovetz, V. Poulin, V. Gluscevic, K. K. Boddy, R. Barkana, and M. Kamionkowski, Tighter limits on dark matter explanations of the anomalous EDGES 21 cm signal, *Phys. Rev. D* **98**, 103529 (2018).
- [36] A. Berlin, D. Hooper, G. Krnjaic, and S. D. McDermott, Severely Constraining Dark Matter Interpretations of the 21-cm Anomaly, *Phys. Rev. Lett.* **121**, 011102 (2018).
- [37] G. D'Amico, P. Panci, and A. Strumia, Bounds on Dark Matter Annihilations from 21 cm Data, *Phys. Rev. Lett.* **121**, 011103 (2018).
- [38] Y. Yang, Contributions of dark matter annihilation to the global 21 cm spectrum observed by the EDGES experiment, *Phys. Rev. D* **98**, 103503 (2018).
- [39] V. Vipp, A. Hektor, and G. Hütsi, Rapid onset of the 21-cm signal suggests a preferred mass range for dark matter particle, *Phys. Rev. D* **103**, 123002 (2021).
- [40] S. Galli, T. R. Slatyer, M. Valdes, and F. Iocco, Systematic uncertainties in constraining dark matter annihilation from the cosmic microwave background, *Phys. Rev. D* **88**, 063502 (2013).
- [41] J. Chluba, Could the cosmological recombination spectrum help us understand annihilating dark matter?, *Mon. Not. R. Astron. Soc.* **402**, 1195 (2010).
- [42] D. T. Cumberbatch, M. Lattanzi, J. Silk, M. Lattanzi, and J. Silk, Signatures of clumpy dark matter in the global 21 cm background Signal, *Phys. Rev. D* **82**, 103508 (2010).
- [43] Y. Yang, Contributions of dark matter annihilation within ultracompact minihalos to the 21 cm background signal, *Eur. Phys. J. Plus* **131**, 432 (2016).
- [44] M. Valdés, A. Ferrara, M. Mapelli, and E. Ripamonti, Constraining DM through 21 cm observations, *Mon. Not. R. Astron. Soc.* **377**, 245 (2007).
- [45] M. Valdés, C. Evoli, A. Mesinger, A. Ferrara, and N. Yoshida, The nature of dark matter from the global high-redshift HI 21 cm signal, *Mon. Not. R. Astron. Soc.* **429**, 1705 (2012).
- [46] J. R. Pritchard and A. Loeb, 21-cm cosmology, *Rep. Prog. Phys.* **75**, 086901 (2012).
- [47] S. Furlanetto, S. P. Oh, and F. Briggs, Cosmology at low frequencies: The 21 cm transition and the high-redshift Universe, *Phys. Rep.* **433**, 181 (2006).
- [48] J. D. Bowman, A. E. E. Rogers, R. A. Monsalve, T. J. Mozdzen, and N. Mahesh, An absorption profile centred at 78 megahertz in the sky-averaged spectrum, *Nature (London)* **555**, 67 (2018).
- [49] A. Cohen, A. Fialkov, R. Barkana, and M. Lotem, Charting the parameter space of the global 21-cm signal, *Mon. Not. R. Astron. Soc.* **472**, 1915 (2017).
- [50] Y. Xu, B. Yue, and X. Chen, Maximum absorption of the global 21 cm spectrum in the standard cosmological model, *Astrophys. J.* **923**, 98 (2021).
- [51] R. F. Bradley, K. Tauscher, D. Rapetti, and J. O. Burns, A ground plane artifact that induces an absorption profile in averaged spectra from global 21-cm measurements with possible application to EDGES, *Astrophys. J.* **874**, 153 (2019).
- [52] R. Hills, G. Kulkarni, P. D. Meerburg, and E. Puchwein, Concerns about modelling of the EDGES data, *Nature (London)* **564**, E32 (2018).
- [53] S. Singh and R. Subrahmanyan, The redshifted 21-cm signal in the EDGES low-band spectrum, *Astrophys. J.* **880**, 26 (2019).
- [54] S. Singh *et al.*, SARAS 2 constraints on global 21-cm signals from the Epoch of Reionization, *Astrophys. J.* **858**, 54 (2018).
- [55] A. Fialkov, R. Barkana, and A. Cohen, Constraining Baryon–Dark Matter Scattering with the Cosmic Dawn 21-cm Signal, *Phys. Rev. Lett.* **121**, 011101 (2018).
- [56] S. Fraser *et al.*, The EDGES 21 cm anomaly and properties of dark matter, *Phys. Lett. B* **785**, 159 (2018).
- [57] A. Hektor, G. Hütsi, L. Marzola, and V. Vaskonen, Constraints on ALPs and excited dark matter from the EDGES 21-cm absorption signal, *Phys. Lett. B* **785**, 429 (2018).
- [58] J. O. Burns *et al.*, Dark cosmology: Investigating dark matter & exotic physics in the dark ages using the redshifted 21-cm global spectrum, [arXiv:1902.06147](https://arxiv.org/abs/1902.06147).
- [59] S. Clark, B. Dutta, Y. Gao, Y.-Z. Ma, and L. E. Strigari, 21 cm limits on decaying dark matter and primordial black holes, *Phys. Rev. D* **98**, 043006 (2018).
- [60] N. Hiroshima, K. Kohri, T. Sekiguchi, and R. Takahashi, Impacts of new small-scale N-body simulations on dark matter annihilations constrained from cosmological 21-cm line observations, *Phys. Rev. D* **104**, 083547 (2021).
- [61] A. Halder and S. Banerjee, Bounds on abundance of primordial black hole and dark matter from EDGES 21-cm signal, *Phys. Rev. D* **103**, 063044 (2021).
- [62] E. D. Kovetz, I. Cholis, and D. E. Kaplan, Bounds on ultralight hidden-photon dark matter from observation of the 21 cm signal at cosmic dawn, *Phys. Rev. D* **99**, 123511 (2019).
- [63] J. R. Bhatt, A. K. Mishra, and A. C. Nayak, Viscous dark matter and 21 cm cosmology, *Phys. Rev. D* **100**, 063539 (2019).
- [64] R. Barkana, N. J. Outmezzuine, D. Redigolo, and T. Volansky, Strong constraints on light dark matter inter-

- pretation of the EDGES signal, *Phys. Rev. D* **98**, 103005 (2018).
- [65] L.-B. Jia and X. Liao, Possible s-wave annihilation for MeV dark matter with the 21-cm absorption, *Phys. Rev. D* **100**, 035012 (2019).
- [66] T. Minoda, S. Yoshiura, and T. Takahashi, Probing isocurvature perturbations with 21-cm global signal in the light of HERA result, *Phys. Rev. D* **105**, 083523 (2022).
- [67] S. Yoshiura, K. Takahashi, and T. Takahashi, Probing small scale primordial power spectrum with 21 cm line global signal, *Phys. Rev. D* **101**, 083520 (2020).
- [68] R. Cen, Constraint on matter power spectrum on 10^6 – $10^9 M_\odot$ scales from τ_e , *Astrophys. J.* **836**, 217 (2017).
- [69] C. T. Byrnes, P. S. Cole, and S. P. Patil, Steepest growth of the power spectrum and primordial black holes, *J. Cosmol. Astropart. Phys.* **06** (2019) 028.
- [70] R. N. Raveendran, K. Parattu, and L. Sriramkumar, Enhanced power on small scales and evolution of quantum state of perturbations in single and two field inflationary models, *Gen. Relativ. Gravit.* **54**, 91 (2022).
- [71] S. Heydari and K. Karami, Primordial black holes ensued from exponential potential and coupling parameter in nonminimal derivative inflation model, *J. Cosmol. Astropart. Phys.* **03** (2022) 033.
- [72] P. Carrilho, K. A. Malik, and D. J. Mulryne, Dissecting the growth of the power spectrum for primordial black holes, *Phys. Rev. D* **100**, 103529 (2019).
- [73] P. S. Cole and J. Silk, Small-scale primordial fluctuations in the 21 cm dark ages signal, *Mon. Not. R. Astron. Soc.* **501**, 2627 (2021).
- [74] S. S. Mishra and V. Sahni, Primordial black holes from a tiny bump/dip in the inflaton potential, *J. Cosmol. Astropart. Phys.* **04** (2020) 007.
- [75] Z. Yi, Q. Gao, Y. Gong, and Z.-h. Zhu, Primordial black holes and scalar-induced secondary gravitational waves from inflationary models with a noncanonical kinetic term, *Phys. Rev. D* **103**, 063534 (2021).
- [76] T.-J. Gao and Z.-K. Guo, Primordial black hole production in inflationary models of supergravity with a single chiral superfield, *Phys. Rev. D* **98**, 063526 (2018).
- [77] S. M. Carroll, W. H. Press, and E. L. Turner, The cosmological constant, *Annu. Rev. Astron. Astrophys.* **30**, 499 (1992).
- [78] A. M. Green, S. Hofmann, and D. J. Schwarz, The first WIMPY halos, *J. Cosmol. Astropart. Phys.* **08** (2005) 003.
- [79] J. M. Bardeen, J. R. Bond, N. Kaiser, and A. S. Szalay, The statistics of peaks of Gaussian random fields, *Astrophys. J.* **304**, 15 (1986).
- [80] M. White, The Zel'dovich approximation, *Mon. Not. R. Astron. Soc.* **439**, 3630 (2014).
- [81] E. Castorina and M. White, Measuring the growth of structure with intensity mapping surveys, *J. Cosmol. Astropart. Phys.* **06** (2019) 025.
- [82] R. A. Porto, L. Senatore, and M. Zaldarriaga, The Lagrangian-space effective field theory of large scale structures, *J. Cosmol. Astropart. Phys.* **05** (2014) 022.
- [83] W. H. Press and P. Schechter, Formation of galaxies and clusters of galaxies by self-similar gravitational condensation, *Astrophys. J.* **187**, 425 (1974).
- [84] S. D. M. White, G. Efstathiou, and C. S. Frenk, The amplitude of mass fluctuations in the Universe, *Mon. Not. R. Astron. Soc.* **262**, 1023 (1993).
- [85] W. J. Percival, The build-up of halos within press-schechter theory, *Mon. Not. R. Astron. Soc.* **327**, 1313 (2001).
- [86] S. Dodelson, in *Modern Cosmology*, edited by S. Dodelson (Academic Press, Burlington, 2003), pp. 261–291.
- [87] P. D. Serpico, E. Sefusatti, M. Gustafsson, and G. Zaharijas, Extragalactic gamma-ray signal from dark matter annihilation: A power spectrum based computation, *Mon. Not. R. Astron. Soc.* **421**, L87 (2012).
- [88] E. Sefusatti, G. Zaharijas, P. D. Serpico, D. Theurel, and M. Gustafsson, Extragalactic gamma-ray signal from dark matter annihilation: An appraisal, *Mon. Not. R. Astron. Soc.* **441**, 1861 (2014).
- [89] W. H. Press and P. Schechter, Formation of galaxies and clusters of galaxies by self-similar gravitational condensation, *Astrophys. J.* **187**, 425 (1974).
- [90] A. A. Abdo *et al.* (Fermi-LAT Collaboration), Constraints on cosmological dark matter annihilation from the Fermi-LAT isotropic diffuse gamma-ray measurement, *J. Cosmol. Astropart. Phys.* **04** (2010) 014.
- [91] J. F. Navarro, C. S. Frenk, and S. D. M. White, A universal density profile from hierarchical clustering, *Astrophys. J.* **490**, 493 (1997).
- [92] L. Zhang, X. Chen, M. Kamionkowski, Z.-g. Si, and Z. Zheng, Constraints on radiative dark-matter decay from the cosmic microwave background, *Phys. Rev. D* **76**, 061301 (2007).
- [93] P. Stöcker, M. Krämer, J. Lesgourgues, and V. Poulin, Exotic energy injection with ExoCLASS: Application to the Higgs portal model and evaporating black holes, *J. Cosmol. Astropart. Phys.* **03** (2018) 018.
- [94] D. Blas, J. Lesgourgues, and T. Tram, The cosmic linear anisotropy solving system (CLASS). Part II: Approximation schemes, *J. Cosmol. Astropart. Phys.* **07** (2011) 034.
- [95] B. Ciardi and P. Madau, Probing beyond the epoch of hydrogen reionization with 21 centimeter radiation, *Astrophys. J.* **596**, 1 (2003).
- [96] M. Kuhlen, P. Madau, and R. Montgomery, The spin temperature and 21 cm brightness of the intergalactic medium in the pre-reionization era, *Astrophys. J.* **637**, L1 (2006).
- [97] H. Liszt, The spin temperature of warm interstellar HI, *Astron. Astrophys.* **371**, 698 (2001).
- [98] P. Villanueva-Domingo, O. Mena, and J. Miralda-Escudé, Maximum amplitude of the high-redshift 21-cm absorption feature, *Phys. Rev. D* **101**, 083502 (2020).
- [99] S. Mittal and G. Kulkarni, Ly α coupling and heating at cosmic dawn, *Mon. Not. R. Astron. Soc.* **503**, 4264 (2021).
- [100] T. Gessey-Jones, N. S. Sartorio, A. Fialkov, G. M. Mirouh, M. Magg, R. G. Izzard, E. d. L. Acedo, W. J. Handley, and R. Barkana, Impact of the primordial stellar initial mass function on the 21-cm signal, *Mon. Not. R. Astron. Soc.* **516**, 841 (2022).
- [101] I. Reis, A. Fialkov, and R. Barkana, The subtlety of Ly α photons: Changing the expected range of the 21-cm signal, *Mon. Not. R. Astron. Soc.* **506**, 5479 (2021).

- [102] J. Mirocha, H. Lamarre, and A. Liu, Systematic uncertainties in models of the cosmic dawn, *Mon. Not. R. Astron. Soc.* **504**, 1555 (2021).
- [103] R. A. Monsalve, A. Fialkov, J. D. Bowman, A. E. E. Rogers, T. J. Mozdzen, A. Cohen, R. Barkana, and N. Mahesh, Results from EDGES high-band: III. New constraints on parameters of the early Universe, *Astrophys. J.* **875**, 67 (2019).
- [104] T. R. Slatyer, Indirect dark matter signatures in the cosmic dark ages. I. Generalizing the bound on s-wave dark matter annihilation from Planck results, *Phys. Rev. D* **93**, 023527 (2016).
- [105] M. Kawasaki, H. Nakatsuka, K. Nakayama, and T. Sekiguchi, Revisiting CMB constraints on dark matter annihilation, *J. Cosmol. Astropart. Phys.* **12** (2021) 015.
- [106] Z. Li, X. Huang, Q. Yuan, and Y. Xu, Constraints on the dark matter annihilation from Fermi-LAT observation of M31, *J. Cosmol. Astropart. Phys.* **12** (2016) 028.
- [107] M. Di Mauro and M. W. Winkler, Multimessenger constraints on the dark matter interpretation of the Fermi-LAT Galactic center excess, *Phys. Rev. D* **103**, 123005 (2021).
- [108] M. Ackermann *et al.* (Fermi-LAT Collaboration), Dark matter constraints from observations of 25 Milky Way satellite galaxies with the Fermi Large Area Telescope, *Phys. Rev. D* **89**, 042001 (2014).
- [109] L. Plice, K. Galal, and J. O. Burns, DARE mission design: Low RFI observations from a low-altitude frozen lunar orbit, [arXiv:1702.00286](https://arxiv.org/abs/1702.00286).
- [110] X. Chen *et al.*, Discovering the sky at the longest wavelengths with small satellite constellations, [arXiv:1907.10853](https://arxiv.org/abs/1907.10853).
- [111] J. Burns *et al.*, Global 21-cm cosmology from the farside of the Moon, [arXiv:2103.05085](https://arxiv.org/abs/2103.05085).
- [112] J. O. Burns, Transformative science from the lunar farside: Observations of the dark ages and exoplanetary systems at low radio frequencies, *Phil. Trans. R. Soc. A* **379**, 20190564 (2020).
- [113] J. Burns *et al.*, A lunar farside low radio frequency array for dark ages 21-cm cosmology, [arXiv:2103.08623](https://arxiv.org/abs/2103.08623).